Effect of Included Solvent Molecules on the Physical Properties of the Paramagnetic Charge Transfer Salts β''-(bedt-ttf)$_4$[(H$_3$O)Fe(C$_2$O$_4$)$_3$]·Solvent (bedt-ttf = Bis(ethylenedithio)tetrathiafulvalene)

Scott S. Turner,*,† Peter Day,*,† K. M. Abdul Malik,‡ Michael B. Hursthouse,‡ Simon J. Teat,§ Elizabeth J. MacLean,§ Lee Martin,†,|| and Samual A. French†

Davy Faraday Research Laboratory, The Royal Institution of Great Britain, 21 Albemarle Street, London, W1X 4BS, UK, Department of Chemistry, Cardiff University, PO Box 912, Cardiff, CF1 3TB, UK, CLRC Daresbury Laboratory, Daresbury, Warrington, Cheshire, WA4 4AD, UK, and Institute for Molecular Sciences, Myodaijicho, Okazaki-shi, Aichi, 444-8585, Japan

Received January 21, 1999

The new charge transfer salt, β''-(bedt-ttf)$_4$[(H$_3$O)Fe(C$_2$O$_4$)$_3$]·C$_5$H$_5$N, **I**, (bedt-ttf = bis(ethylenedithio)tetrathiafulvalene) has a crystal structure closely similar to that of the reported salt β''-(bedt-ttf)$_4$[(H$_3$O)Fe(C$_2$O$_4$)$_3$]·C$_6$H$_5$CN, **II**, which has a superconducting critical temperature of 8.6 K. However, variable temperature magnetic and transport experiments show that **I** has a metal to insulator transition at 116 K. The crystal structure of **I** has been determined above (150 K) and below (90 K) the metal to insulator transition and comparisons are made with the structure of **II**. The pyridine solvate crystallizes in the monoclinic space group $C2/c$ with $a = 10.267(2)$ Å, $b = 19.845(4)$ Å, $c = 34.907(7)$ Å, $\beta = 93.22(3)°$, $Z = 4$ at 150 K and with $a = 10.2557(15)$ Å, $b = 19.818(28)$ Å, $c = 34.801(49)$ Å, $\beta = 93.273(14)°$, $Z = 4$ at 90 K. The structures of **I** and **II** both consist of layers of bedt-ttf with +0.5 formal charge per molecule and layers of approximately hexagonal symmetry containing H_3O^+ and $[Fe(C_2O_4)_3]^{3-}$. The solvent molecules occupy hexagonal cavities formed by the anionic layer. Changing the solvent molecule from C$_6$H$_5$CN to C$_5$H$_5$N induces disorder in the bedt-ttf layer which accounts for the dramatic difference in observed physical properties. For **I**, at 150 K, one-half of all the bedt-ttf molecules have identical conformations to all the molecules in **II** where both terminal ethylene groups of each bedt-ttf molecule are twisted and eclipsed with respect to the opposite end of the molecule. The remaining 50% of bedt-ttf molecules in **I** have disordered ethylene groups. The disorder persists at 90 K where it can be resolved into two conformations: twisted-twisted eclipsed and twisted-twisted staggered.

Introduction

Salts of the organic donor molecule bis(ethylenedithio)-tetrathiafulvalene, bedt-ttf, exhibit a range of ground states from highly conducting metallic or superconducting states to wide band gap semiconducting and insulating (e.g., CDW, SDW, Spin-Peierls).[1] It has been almost two decades since the discovery of superconductivity in organic radical cation salts[2] and subsequently it has been found that the superconducting critical temperature, T_c, and indeed the overall type of conducting behavior, can be profoundly influenced by the counterion.[1] Furthermore, a linear relationship between T_c and effective volume, V_{eff}, has been determined,[3] where V_{eff} is a function of unit cell volume, anion volume, and the number of conduction electrons in the unit cell.

Typically the structures of bedt-ttf charge transfer salts consist of stacks of positively charged bedt-ttf molecules built into layers, by lateral close contacts between S atoms, which are interleaved by layers of the counterions. The bedt-ttf molecules pack in a variety of ways leading to phases which for 2:1 (bedt-ttf:anion) salts are designated by the letters α, β, γ, κ, etc. The majority of those salts which exhibit superconductivity have the κ packing motif. For example, the series with formula κ-(bedt-ttf)$_2$Cu[N(CN)$_2$]X contains the salt with the highest T_c under ambient conditions (X = Br, $T_c = 11.8$ K) and that with the highest T_c so far found in the bedt-ttf salts (X = Cl, T_c = 12.8 K at 0.3 kbar).[4,5] It was therefore pertinent to investigate factors which influence the donor packing motif and promote formation of the κ phase. A plausible rationalization for the occurrence of κ type packing in κ-(bedt-ttf)$_2$Cu(CN)[N(CN)$_2$], κ'-(bedt-ttf)$_2$Cu$_2$(CN)$_3$, and the κ-type salts of I_3^- is based on the concept of "docking" terminal ethylene hydrogen atoms of the bedt-ttf into a regular array of empty cavities provided by arrangement of the counterions.[6] Emphasis was placed on the

* Corresponding author. E-mail: sst@ri.ac.uk, pday@ri.ac.uk.
† Davy Faraday Research Laboratory.
‡ University of Cardiff.
§ CLRC Daresbury Laboratory.
|| Institute for Molecular Science.

(1) Williams, J. M.; Ferraro, J. R.; Thorn, R. J.; Carlson, K. D.; Geiser, U.; Wang, H. H.; Kini, A. M.; Whangbo, M. H. *Organic Superconductors (Including Fullerenes): Synthesis, Structure, Properties and Theory*; Prentice Hall: Englewood Cliffs, NJ, 1992.
(2) Jérome, D.; Mazaud, A.; Ribault, M.; Bechgaard, K. *J. Phys. Lett.* **1980**, *41*, L95.
(3) Saito, G.; Urayama, H.; Yamochi, H.; Oshima, K. *Synth. Met.* **1988**, *A33*, 27.
(4) Kini, A. M.; Geiser, U.; Wang, H. H.; Carlson, K. D.; Williams, J. M.; Kwok, W. K.; Van Der Voort, K. G.; Thompson, J. E.; Stupka, D. L.; Jung, D.; Whangbo, M. H. *Inorg. Chem.* **1990**, *29*, 2555.
(5) Williams, J. M.; Kini, A. M.; Wang, H. H.; Carlson, K. D.; Geiser, U.; Montgomery, L. K.; Pyrka, G. J.; Watkins, D. M.; Kommers, J. M.; Boryschuk, S. J.; Crouch, A. V. S.; Kwok, W. K.; Schirber, J. E.; Overmyer, D. L.; Jung, D.; Whangbo, M. H. *Inorg. Chem.* **1990**, *29*, 3272.

10.1021/ic990102u CCC: $18.00
Published on Web 07/02/1999

shape and size of the anion cavities and on short atomic contacts between neighboring donors across an anionic layer. The effect on the collective electronic properties of changing included neutral molecules, such as solvent molecules, as a means of modulating the unit cell volume and packing of donor molecules has not been widely studied. Members of the three component series κ-(bedt-ttf)$_2$M(CF$_3$)$_4$·(1,1,2-trihaloethane) with M = Cu, Ag have been made with several different solvents and all have a superconducting state with T_c ranging from 2.6 to 11.1 K.[7−9] The molecular conductor (bedt-atd)$_2$PF$_6$·(THF), based on a nonplanar donor, is metallic; but replacement of the anion with BF$_4$ or the solvent with 2,5-dihydrofuran induces a metal−insulator transition at 200 and 150 K, respectively.[10] A series of single crystals of (bedt-ttf)$_4$Re$_6$Se$_5$Cl$_9$·[guest], guest = DMF, THF, dioxane, have been prepared.[11] All four compounds have the same layered organization with the guest molecules incorporated at a single site at the cation−anion interface and all are metallic at high temperatures. However, their electrical conductivity at low temperatures depends strongly upon the size, shape, and symmetry of the neutral guest molecule.

Recently we reported the first molecular superconductor containing paramagnetic d-block ions: β''-(bedt-ttf)$_4$[(H$_3$O)Fe(C$_2$O$_4$)$_3$]·C$_6$H$_5$CN, **II**,[12,13] and its Cr(III) analogue.[14] These salts have the alternating donor−acceptor structure and in both compounds the templating effect of the benzonitrile solvent plays an important role in stabilizing the structure by occupying an approximately hexagonal cavity in the anionic acceptor layer. It can be expected that minor changes made to the solvent moiety would preserve the overall β''-phase structure but slightly modify lattice parameters and intermolecular interactions. Here we report that replacing benzonitrile by pyridine in **II** gives rise to β''-(bedt-ttf)$_4$[(H$_3$O)Fe(C$_2$O$_4$)$_3$]·C$_5$H$_5$N, **I**, whose crystal structure differs only in fine detail from that of **II** but which shows distinctly different magnetic and transport properties.

Experimental Section

Bedt-ttf was prepared as previously published,[15] 18-crown-6 was purchased from Aldrich, and racemic [NH$_4$]$_3$[Fe(C$_2$O$_4$)$_3$]·3H$_2$O was prepared by literature methods.[16] All materials and equipment were carefully cleaned prior to use. 18-crown-6 was treated by mixing with dry MeCN, isolating the solid and drying in vacuo. Bedt-ttf was recrystallized three times from dry CHCl$_3$ and [NH$_4$]$_3$[Fe(C$_2$O$_4$)$_3$]·3H$_2$O was recrystallized four times from H$_2$O. Pyridine was purified by literature methods.[17] The electrochemical cell was cleaned with concentrated HNO$_3$ followed by several washes with H$_2$O then dried over 2 days at 140 °C.

Table 1. Crystallographic Data for **I** and **II** at 150 K and for **I** at 90 K

	I		**II**
empirical formula	$C_{48.5}H_{36.5}FeN_{0.5}O_{13}S_{32}$	$C_{51}H_{32}FeNO_{13}S_{32}$	$C_{53}H_{39}FeNO_{13}S_{32}$
a, Å	10.267(2)	10.2557(15)	10.232(12)
b, Å	19.845(4)	19.818(3)	20.04(3)
c, Å	34.907(7)	34.801(5)	34.97(2)
β, deg	93.22(3)	93.273(4)	93.25(11)
V, Å^3	7101.0	7061.8	7157
Z	4	4	4
fw	1916.05	1948.55	1979.78
space group	*C*2/*c* (No. 15)	*C*2/*c* (No. 15)	*C*2/*c* (No. 15)
T, K	150(2)	90(2)	150(2)
λ, Å	0.710 69, Mo Kα	0.688 30, synchrotron	0.710 69, Mo Kα
ρ_{calcd}, g cm^{-3}	1.792	1.833	1.835
μ, cm^{-1}	12.13	12.21	12.07
$R(F_o)^a$	0.0606	0.1240	0.0416
$R_w(F_o^2)^b$	0.1657	0.2952	0.0760

^{a} $R = \sum(F_o - F_c)/\sum F_o$. ^{b} $R_w = \{\sum[w(F_o^2 - F_c^2)^2]/\sum[w(F_o^2)^2]\}^{1/2}$.

Synthesis of β''-(bedt-ttf)$_4$[(H$_3$O)Fe(C$_2$O$_4$)$_3$]·C$_5$H$_5$N, I. Crystals of **I** were grown by electrocrystallization from solutions in H-shaped cells in which the Pt anode and cathode (rods; 1 mm diameter, 15 mm length) were separated by two permeable membranes to prevent contamination by reduction products. A constant current of 0.5 μA was applied across the cell in the dark at a constant temperature of 20 °C using purified pyridine (40 mL) containing two drops of H$_2$O as the solvent. The supporting electrolyte was racemic [NH$_4$]$_3$[Fe(C$_2$O$_4$)$_3$]·3H$_2$O (100 mg) with 18-crown-6 (200 mg) added for dissolution, and solid bedt-ttf (10 mg) was placed in the base of the anode arm of the H-cell. Dark brown to black hexagonal shaped plates began to grow on the Pt anode after 4 days, at which point the current was increased to 1.0 μA. Growth was stopped after 2 weeks when between 3 and 5 mg of **I** was collected, washed with acetone, and air-dried. Product from several cells was necessary for subsequent physical investigations.

Crystal Structure Determination. Crystallographic data were recorded at 150 K by a Delft Instruments FAST TV area detector diffractometer using Mo Kα radiation, following previously described procedures.[18] The structure of **I** was solved by direct methods (SHELXS86)[19] and difference electron density synthesis, and refined on F^2 by full-matrix least-squares (SHELXL93)[20] using all unique data. At 150 K the pyridine solvate was located on the 2-fold symmetry axis with only half being present per metal oxalate. The H atoms were included in calculated positions using the Riding model.

The crystallographic data at 90 K were collected using the microcrystal diffraction facility on station 9.8 of the synchrotron radiation source, CLRC Daresbury Laboratory. Data collection was achieved with a Siemens SMART CCD diffractometer. The structure was solved by direct methods, as above, and refined on F^2 by full-matrix least-squares. The crystallographic data, conditions for the collection of intensity data, and some features of the structure refinements are listed in Table 1 for **I** at 150 and 90 K and are reproduced for **II** to facilitate comparison. Relevant bedt-ttf atomic distances are presented in Table 2.

Physical Measurements. Magnetic susceptibility measurements were performed with a Quantum Design MPSM7 SQUID magnetometer using 19.01 mg of randomly orientated polycrystalline material encased in a gel capsule. Magnetization was recorded from 2 to 300 K and magnetization measurements at 2 K were made between 0 and 7 T. Four probe DC transport measurements on single crystals were measured from 300 to 65 K by the standard four probe method with an Oxford Instruments Mag-Lab 2000 equipped with an EP probe. The

(6) Yamochi, H.; Tokutaro, K.; Matsukawa, N.; Saito, G.; Takehiko, M.; Kusunoki, M.; Sakaguchi, K. *J. Am. Chem. Soc.* **1993**, *115*, 11319.
(7) Schlueter, J. A.; Williams, J. M.; Geiser, U.; Dudek, J. D.; Kelly, M. E.; Sirchio, S. A.; Carlson, K. D.; Naumann, D.; Roy, T.; Campana, C. F. *Adv. Mater.* **1995**, *7*, 634.
(8) Schlueter, J. A.; Williams, J. M.; Geiser, U.; Wang, H. H.; Kini, A. M.; Kelly, M. E.; Dudek, J. D.; Naumann, D.; Roy, T. *Mol. Cryst. Liq. Cryst. A* **1996**, *285*, 43.
(9) Geiser, U.; Schlueter, J. A.; Williams, J. M.; Kini, A. M.; Dudek, J. D.; Kelly, M. E.; Naumann, D.; Roy, T. *Synth. Met.* **1997**, *85*, 1465.
(10) Imaeda, K.; Krober, J.; Nakano, C.; Tomura, M.; Tanaka, S.; Yamashita, Y.; Kobayashi, H.; Inokuchi, H.; Kobayashi, A. *Mol. Cryst. Liq. Cryst. A* **1997**, *296*, 205.
(11) Pénicaud, K.; Boubekeur, K.; Batail, P.; Canadell, E.; Auban-Senzier, P.; Jérome, D. *J. Am. Chem. Soc.* **1993**, *115*, 4101.
(12) Graham, A. W.; Kurmoo, M.; Day P. *J. Chem. Soc., Chem. Commun.* **1995**, 2061.
(13) Kurmoo M.; Graham A. W.; Day P.; Coles S. J.; Hursthouse M. B.; Caulfield J. L.; Singleton J.; Pratt F. L.; Hayes W.; Ducasse L.; Guionneau P. *J. Am. Chem. Soc.* **1995**, *117*, 12209.
(14) Martin, L.; Turner, S. S.; Day, P.; Mabbs, F. E.; McInnes, E. J. L. *J. Chem. Soc., Chem. Commun.* **1997**, 1367.
(15) Larsen, J.; Lenoir, C. *Synthesis* **1988**, *2*, 134.
(16) Bailar, J. C.; Jones, E. M. *Inorg. Synth.* **1993**, *1*, 35.
(17) Perrin, D. D.; Armarego, W. L. F. *Purification of Laboratory Chemicals*; Pergammon Press: Oxford, UK, 1989.
(18) Darr, J. A.; Drake, S. R.; Hursthouse, M. B.; Malik, K. M. A. *Inorg. Chem.* **1993**, *32*, 5704.
(19) Sheldrick, G. M. *Acta Crystallogr.* **1990**, *A46*, 467.
(20) Sheldrick, G. M. *SHELXL93: Program for Crystal Refinement*; University of Göttingen, Göttingen, Germany, 1993.

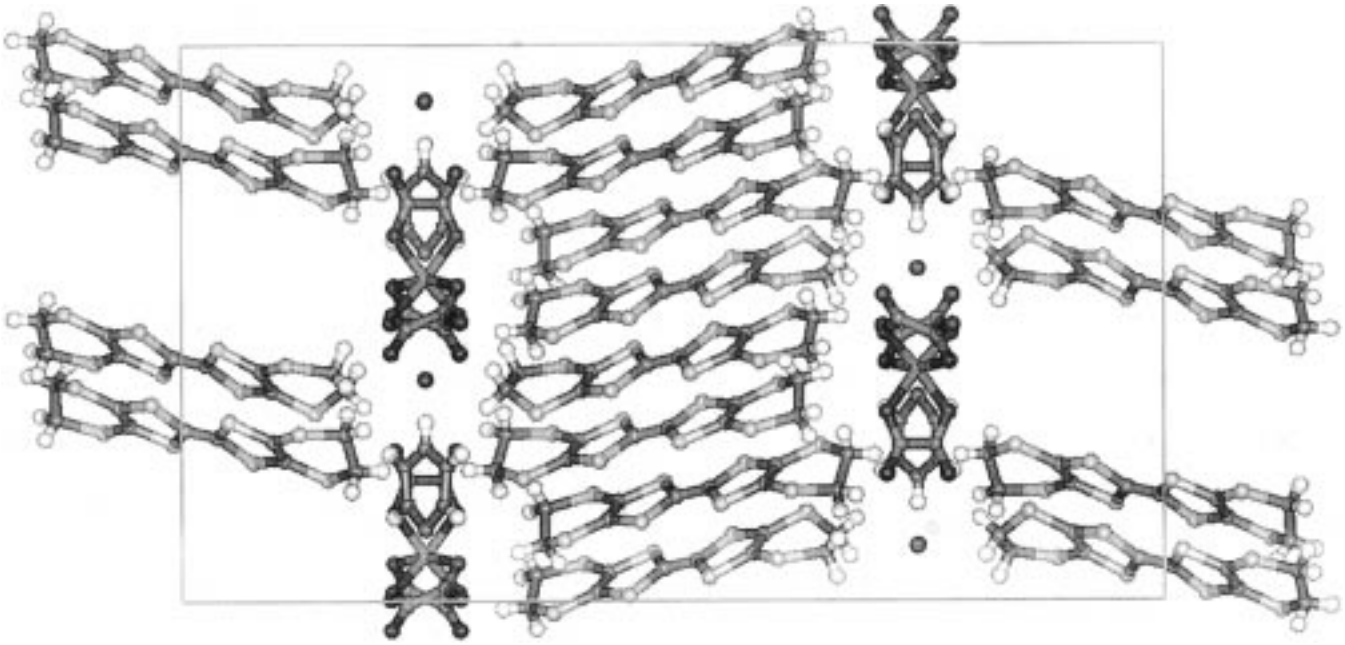

Figure 1. Crystal structure of **I** projected along the *b* axis.[28]

Table 2. Selected Atomic Distances (Å) for Bedt-ttf in **I** at 150 and 90 K

Inner bedt-ttf Atomic Distances of **I** at 150 K			
C1−C6	1.352(11)	C11−C16	1.348(11)
C6−S6	1.739(8)	C16−S14	1.740(7)
S6−C7	1.745(8)	S14−C17	1.729(9)
C7−C10	1.353(11)	C17−C20	1.355(11)
C10−S5	1.743(8)	C20−S13	1.750(8)
S5−C6	1.737(8)	S13−C16	1.752(8)
C1−S2	1.733(8)	C11−S10	1.729(8)
S2−C2	1.737(8)	S10−C12	1.747(8)
C2−C5	1.357(11)	C12−C15	1.335(11)
C5−S1	1.728(8)	C15−S9	1.733(8)
S1−C1	1.747(7)	S9−C11	1.745(7)
Inner bedt-ttf Atomic Distances of **I** at 90 K			
C(1)−C(6)	1.348(14)	C(11)−C(16)	1.353(14)
C(6)−S(6)	1.740(11)	C(16)−S(14)	1.755(10)
S(6)−C(7)	1.746(10)	S(14)−C(17)	1.736(10)
C(7)−C(10)	1.387(13)	C(17)−C(20)	1.370(13)
C(10)−S(5)	1.736(10)	C(20)−S(13)	1.748(9)
S(5)−C(6)	1.745(10)	S(13)−C(16)	1.730(10)
C(1)−S(2)	1.738(10)	C(11)−S(10)	1.746(10)
S(2)−C(2)	1.749(11)	S(10)−C(12)	1.747(10)
C(2)−C(5)	1.351(14)	C(12)−C(15)	1.331(13)
C(5)−S(1)	1.741(10)	C(15)−S(9)	1.748(9)
S(1)−C(1)	1.746(9)	S(9)−C(11)	1.735(11)

measurement contacts were attached to the flat hexagonal faces of single crystals with Pt paste, measuring in the most conductive *b* direction of the hexagonal plane. Raman spectra of single crystals were recorded at room temperature in reflectance mode by a Renshaw Raman imaging microscope equipped with a He−Ne laser (632.6 nm). Spectra were measured with the polarization of the incident laser beam parallel to the *b* crystal direction. Scan time was 300 s and spectra were centered at 1400 cm^{-1}.

Results

Description of the Structure of β''-(bedt-ttf)$_4$[$(H_3O)Fe(C_2O_4)_3$]·C_5H_5N, I, at 150 K and 90 K. The pyridine solvate **I** is all but isostructural with the superconductor β''-(bedt-ttf)$_4$[$(H_3O)Fe(C_2O_4)_3$]·C_6H_5CN,[12,13] **II**. Both structures consist of alternating layers of bedt-ttf cations and layers containing $[Fe(C_2O_4)_3]^{3-}$, H_3O^+, and the templating solvent. Figure 1 shows the layered structure of **I** projected along the *b* axis, and Figure 2 shows the atom labeling scheme with anisotropic thermal ellipsoids at 150 K. The cation layers adopt a β'' packing arrangement with stacks of bedt-ttf molecules having numerous short intermolecular S···S distances closer than the sum of sulfur van der Waals radii (3.6 Å). For the benzonitrile salt these range from 3.3 to 3.59 Å and for the pyridine salt 3.34−3.6 Å, that is with no significant difference. In both cases the oxalate-containing layers have a honeycomb arrangement of $[Fe(C_2O_4)_3]^{3-}$ ions where the terminal O atoms of the oxalate are hydrogen bonded to the hydroxonium molecule. The O−H(H_3O)··· O(oxalate) distance is measured for **I** at 1.87 Å whereas for **II** the H atoms of H_3O^+ are not found and the O(H_3O)···O(oxalate) distances are 2.8−2.9 Å. Thus an array of hexagonal cavities is formed within the anionic layer, bounded by alternate intralayer O(H_3O^+) and Fe atoms. A single anionic layer contains exclusively one chiral form of $[Fe(C_2O_4)_3]^{3-}$ (D_3 point symmetry) with the next nearest layer containing only the other enantiomer. This gives an anionic layer pattern of Δ−Λ−Δ−Λ... throughout the structure. In **II** the solvent molecules are totally ordered and occupy the hexagonal cavities with the −C≡N functional groups all oriented parallel to the *b* axis and directed toward an Fe center. The pyridine solvate, **I**, crystallizes in the same space group as **II** but in this case the N atoms of the pyridine molecules, still aligned along the *b* axis and fully ordered, point toward the O atom of a hydroxonium molecule at the opposite end of the cavity. The N(pyridine)···O(H_3O) distance is 4.6 Å which is too long to be considered as a close contact. However, close contacts do occur between the solvent and surrounding oxalate ligand. In **I** the pyridine protons at positions 3 and 5 are 2.7 Å from a terminal O (oxalate) atom and in **II** the protons at positions 2 and 6 are 2.6 Å from a similar O atom. These should be considered as only weak van der Waals interactions and certainly not C−H···O hydrogen bonds, which are rare and only found in conjugated systems where the proton is sufficiently acidic. Nevertheless these weak contacts are cumulative and probably confer some stability and promote the solvent templating effect. In both solvates the planes of the solvent molecules are tilted about the *b* axis with respect to a plane described by uppermost oxygen atoms in a $[Fe(C_2O_4)_3]^{3-}$ unit, the tilt angle being 32.9° in **II** and 36.1° in

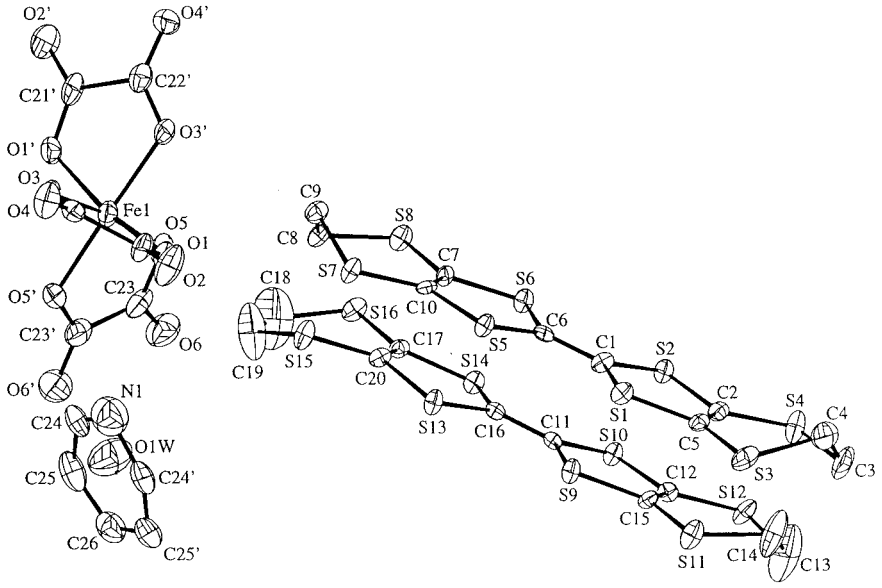

Figure 2. Asymmetric unit of **I** at 150 K showing 50% thermal ellipsoids and atom numbering scheme.

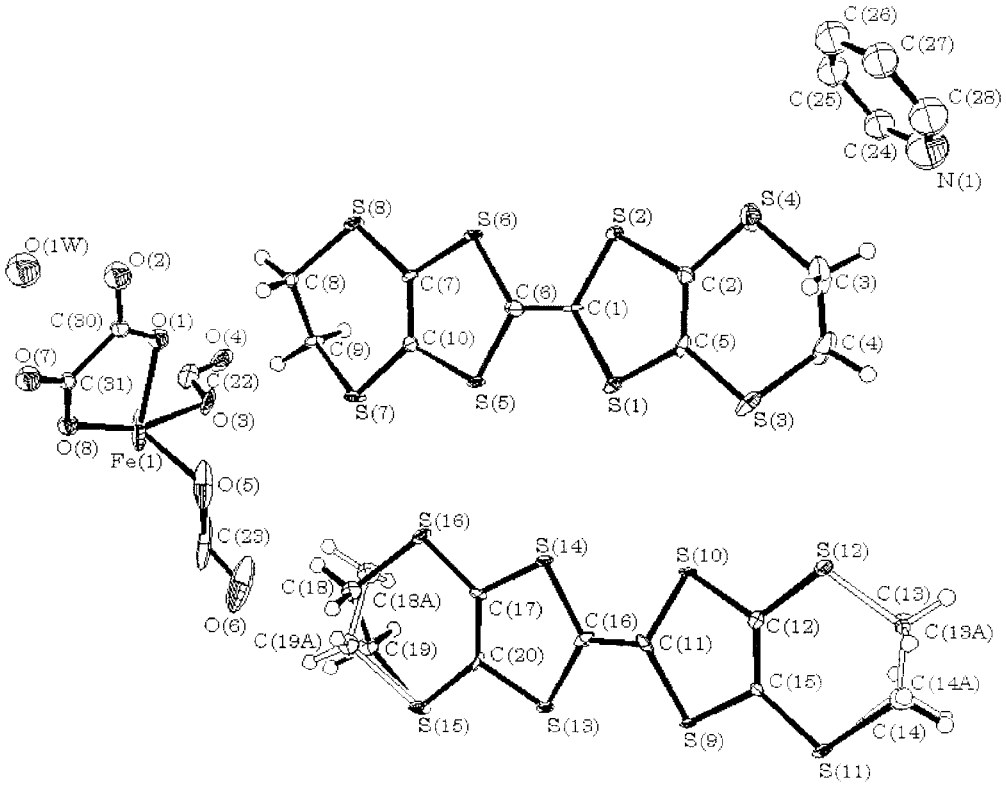

Figure 3. Asymmetric unit of **I** at 90 K showing 50% thermal ellispsoids and atom numbering scheme.

I. In both cases the solvent tilt corresponds to the tilt of two bidentate oxalate ligands at opposite edges of the hexagonal cavity. The matching tilt promotes the close contacts between the H (solvent) and O (oxalate) atoms described above.

On either side of the anionic layers containing the oxalato ligands lie layers containing bedt-ttf donor molecules. H atoms on the terminal CH_2 groups in each bedt-ttf molecule lie close to O atoms of the oxalate ligands in the sandwiching anionic layers. The bedt-ttf molecules in **I**, at 150 K, fall into two distinct groups: those with a twisted-twisted conformation and those where one end is twisted and the other is unresolved at this temperature (see Discussion section). To isolate the nature of this disorder, the structure of **I** was refined at 90 K and Figure 3, which shows the atom labeling scheme and thermal ellipsoids at the lower temperature, reveals subtle differences between this structure and that at 150 K. The main difference resides in the positions of the C atoms of the previously disordered ethylene groups, which are now refined into two distinct sites. Another difference occurs in the $Fe(C_2O_4)_3$ unit. In the 150 K structure, three half oxalate groups were located with symmetry generating the whole molecules but at 90 K one of the oxalate groups is a whole group with half occupancy. The overall stoichiometry is therefore not affected. It is possible that the same sort of disorder is occurring for O(5), C(23), and O(6). The relatively large structure factors for these atoms indicate that disorder is likely. Similar differences appear for the pyridine molecule thus explaining the slight difference in empirical formulas given in Table 1. At 150 K the pyridine was located on a 2-fold axis

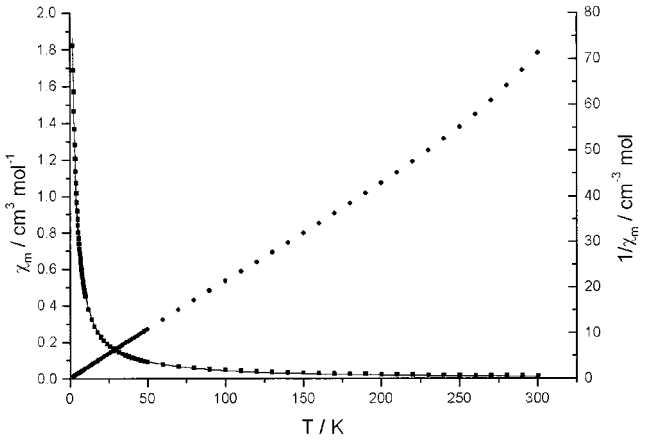

Figure 4. Temperature variation of susceptibility and inverse susceptibility for **I**.

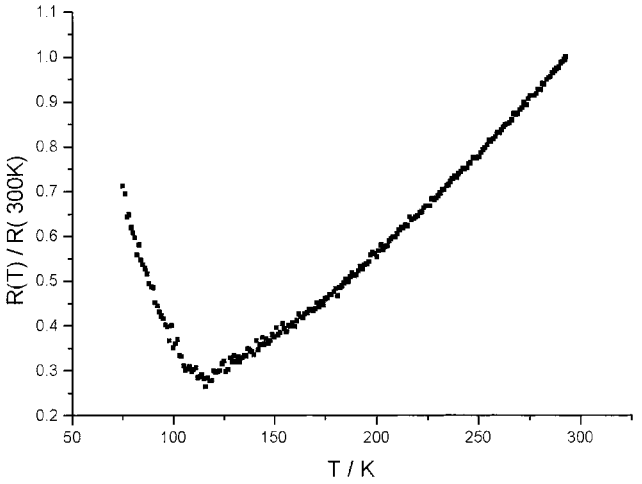

Figure 5. Temperature variation of four-probe DC resistance for **I**.

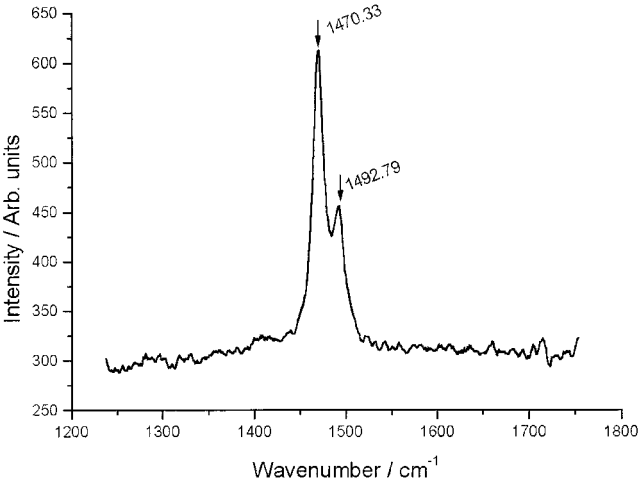

Figure 6. Room-temperature reflectance Raman spectrum for **I**.

but at 90 K a whole pyridine molecule was located with half occupancy. Using the distances in Table 2, bond length analysis[21] reveals little difference between the bedt-ttf charges at 150 K and at 90 K, and with those at room temperature. For the two crystallographically independent bedt-ttf molecules the calculated charges are +0.48, and +0.60 at 150 K; and +0.49, and +0.60 at 90 K. There is also the distinct possibility that some loss of crystallinity below the metal−insulator transition temperature accounts for the relatively high final discrepancy values at 90 K.

Magnetic Properties. Figure 4 shows the temperature dependence of the molar susceptibility and inverse susceptibility of **I** measured in an applied field of 0.1 T. The molar susceptibility, corrected for core diamagnetism, was fitted to a Curie−Weiss expression from 300 to 2 K together with a temperature independent contribution due to Pauli paramagnetism from the conduction electrons. The measured Curie constant of 4.89 emu K mol^{-1} can be compared with the expected value of 4.377 emu K mol^{-1} for high spin Fe(III). A small negative Weiss constant of −0.04 K is also observed and the calculated Pauli contribution was 0.006 cm^3 mol^{-1}. Figure 4 also gives the susceptibility fitted to a curve, calculated with these parameters and shown as a solid line over the experimental data. When the sample is cooled under zero applied field followed by measuring the temperature dependence of magnetization in 0.5mT from 2 to 30 K, no Meissner effect is observed. Field dependent magnetization measurements at 2 K gave a saturation value of 5.2 Nβ at 7 T, ideal for high spin Fe(III). **II** has similar Curie−Weiss behavior at moderate external fields (>100 G) but at low fields the Meissner effect is seen below 8.6 K.[12,13]

Transport Properties. The resistivity of **I** decreases with temperature as for a metal from a value of $\sim 10^{-2}$ Ω cm at 200 K, but at 116 K there is a very sharp increase in resistance indicating a metal−insulator transition (Figure 5). This behavior is in striking contrast to that of **II**, which is also metallic, again with resistivity $\sim 10^{-2}$ Ω cm at 200 K, but remains metallic down to 8.6 K, below which it behaves as a type II superconductor.[12,13] Neither in **I** nor **II** does the transport show hysteresis on slow cooling and heating at 0.5 degrees per minute.

Raman Spectroscopy. A fundamental issue in the field of molecular charge transfer salts is the determination of the formal charge on the donor molecules. In neutral salts a simple calculation based on the charges on the counterion divided by the number of cationic donor molecules will suffice. However, in some situations the anionic charge may be ambiguous or X-ray diffraction studies are unable to deduce the exact nature of the anion. In the present case, the question arises as to whether the water molecules in **I** and **II** are present as H_2O or H_3O^+. The difference is important since it affects the filling of the conduction band and hence the Fermi surface energy. A useful technique for determining the partial charges of the cations in bedt-ttf salts relies on an empirical correlation based on C=C and C−S bond lengths within the ttf core of the bedt-ttf molecule[21] and results of this analysis are given above. Another means of obtaining such information is available by recording the C=C and C−S vibrational modes in the crystals by Raman spectroscopy. By analogy with charge determination using bond lengths, the vibrational frequencies can be correlated with those of charge transfer salts where the formal charge of the cation is well defined. The two totally symmetric (Raman active) C=C stretching modes between 1400 and 1550 cm^{-1} are particularly sensitive to the charge state of the donor molecule. The room temperature spectrum of **I** shows two distinct absorption frequencies (Figure 6) at 1470 and 1493 cm^{-1}. By comparison to literature values[22] these frequencies indicate a charge of +0.5 on each donor molecule, which is only consistent with overall charge neutrality in the lattice if at least the majority of the water is present as H_3O^+.

(21) Guionneau, P.; Kepert, C. J.; Bravic, G.; Chasseau, D.; Truter, M. R.; Kurmoo, M.; Day, P. *Synth. Met.* **1997**, *86*, 1973.

(22) Wang, H. H.; Ferraro, J. R.; Williams, J. M.; Geiser, U.; Schlueter, J. A. *J. Chem. Soc., Chem. Commun.* **1994**, 1893.

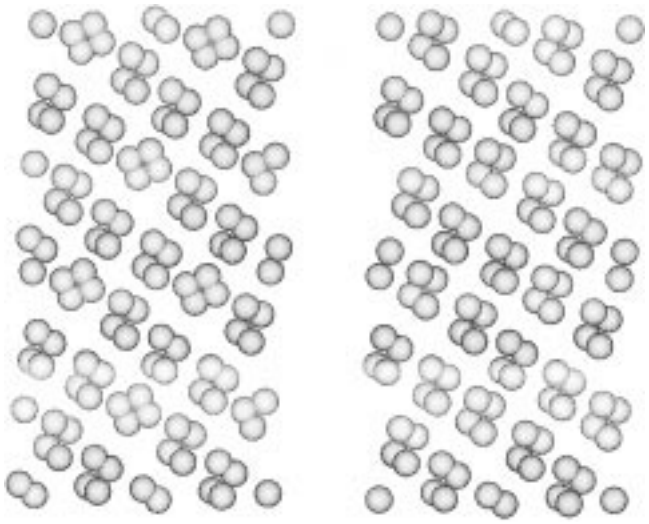

Figure 7. Positions of H atoms on one side of a plane of bedt-ttf at 150 K for **I** (left) and **II** (right).

Discussion

To understand the origin of the striking difference between the magnetic and transport properties of **I** and **II** requires closer comparison of their crystal structures. Direct comparison may be made possible between the structures where both are in their metallic regime. The smaller volume of the pyridine molecule in **I** compared to the benzonitrile molecule in **II** does not lead to a correspondingly smaller size of the hexagonal cavity. The size of the cavity is essentially controlled by the hydrogen bonding between H_3O^+ and terminal O (oxalate) atoms rather than by the volume of the solvent molecule. Expressed in terms of distance between Fe and O (H_3O), which bound the hexagonal cavity, the area of the solvent cavity is 101.8 Å^2 in **I** and 102.5 Å^2 in **II**. The only significant difference in the anion networks for the two solvates is that in **II** the solvent cavity is almost completely filled while in **I** a small unoccupied volume remains due to the absence of the $-C\equiv N$ group.

It is thought that weak H-bonds and/or steric effects between the terminal CH_2 groups and the inorganic layer significantly influence the stacking arrangement of the bedt-ttf and hence determine the transport properties of this class of charge-transfer salt.[23] Evidence for such interaction here comes from translation of the $[Fe(C_2O_4)_3]^{3-}$ units within the plane of the anion layer on passing from one layer to the next. Displacement of $[Fe(C_2O_4)_3]^{3-}$ matches the tilt of the intervening bedt-ttf molecules so that the contacts between H (CH_2) and O (oxalate) are identical at both ends of each bedt-ttf molecule. Planes described by the central ttf-like unit of bedt-ttf in **I** are thus oriented at 68.5° to planar O (oxalate) atoms. To visualize this interaction better we can look at an isolated array of H atoms from the terminal CH_2 groups, which lie at one end of an array of bedt-ttf stacks, and which therefore form the interface with the oxalate layer. Figure 7 (right) shows these H atoms for the superconductor, **II**. Comparison with the analogous set of H atoms for the nonsuperconducting material, **I**, Figure 7 (left), reveals that while three-quarters of the groups of atoms are organized in exactly the same way as in the superconductor, the fourth is different. In the superconductor all the terminal $-CH_2CH_2-$ have the same twisted conformation (eclipsed with respect to those at the other end of the bedt-ttf molecule) and so fit together neatly into stacks. In contrast, in **I**, only three-quarters of the bedt-ttf molecules have this twisted and eclipsed configuration, while in the remainder the $-CH_2CH_2-$ groups are twisted at one end but have an unresolved conformation at the other. The protons in question are bonded to C atoms that have high anisotropic displacement parameters relative to the other C atoms of bedt-ttf. Examining the relative positions of the unresolved CH_2 units and the inorganic layer shows the probable origin of this difference: the unresolved-twisted molecule in each stack lies above the hexagonal solvent cavity in the anion layer with the unresolved end being above the gap remaining when pyridine replaces benzonitrile. The presence of C atoms with high displacement parameters in **I** indicates the presence of static or dynamic disorder in **I** but not in **II**. At 298 K significant thermal motion may exist in at least one ethylene group of all the bedt-ttf molecules in the unit cell,[24] though they are commonly ordered at the temperatures used in the present experiment.[24,25] High quality single point energy Density Functional Calculations have been performed on the two crystallographically different bedt-ttf molecules in **I** and **II** using the DMol^3 code.[26] The generalized gradient corrected functional derived by Perdew and Wang[27] was used in conjunction with double numeric basis set with polarization. The calculations support the assertion that the conformation of the bedt-ttf molecule in **I** is an artifact of crystallographic disorder as it is 2.17 eV higher in energy than that in **II**. When the structure of **I** was fully optimized using standard minimization techniques the structure relaxed to that of **II**. Details of this treatment will be published separately. Furthermore, if the centroid of the refined electron density of the unresolved C atoms is a true representation of the mean positions, then the unresolved-twisted molecule would also be highly strained, with $S-C(CH_2)-C(CH_2)$ angles at the unresolved end being 124.7° and 128.4°, whereas those for the twisted end range from 112.9° to 115.7° compared to 109.4° for an idealized tetrahedral angle. These results confirm that either static or dynamic disorder is operating in **I** at 150 K in the metallic regime. At 90 K, in the insulator regime, the ethylene disorder persists but can now be resolved.

Conclusions

In summary, we have found that substituting benzonitrile, which plays an important role as a template in forming the structure of the paramagnetic molecular superconductor, **II**, by pyridine, produces a phase, **I**, which crystallizes in the same space group with closely similar cell parameters and has similar metallic properties at room temperature to **II**, but which has a metal-to-insulator transition at 116 K. When both materials are in their metallic regimes, they have the β''-(bedt-ttf) packing motif but in the pyridine solvate one-quarter of the bedt-ttf have an unresolved−twisted conformation in contrast with the superconducting phase **II** where they are all twisted−twisted and eclipsed with relatively low thermal parameters. All bond distances and angles within the anionic layers are closely similar in the two compounds except that in **I** there is a void in each hexagonal cavity, corresponding to the position of the unresolved

(23) Martin, L.; Turner, S. S.; Day, P.; Malik, K. M. A.; Coles, S. J.; Hursthouse, M. B. *J. Chem. Soc., Chem. Commun.* **1999**, 513.

(24) Emge, T. J.; Wang, H. H.; Leung, P. C. W.; Rust, P. R.; Cook, J. D.; Jackson, P. L.; Carlson, K. D.; Williams, J. M.; Whangbo, M. H.; Venturini, E. L.; Schriber, J. E.; Azevedo, L. J.; Ferraro, J. R. *J. Am. Chem. Soc.* **1986**, *108*, 695 and references therein.

(25) Laukhina, E. E.; Narymbetov, B. Z.; Zorina, L. V.; Khasanov, S. S.; Rozenberg, L. P.; Shibaeva, R. P.; Buravov, L. I.; Yagubskii, E. B.; Avramenko, N. V.; Van, K. *Synth. Met.* **1997**, *90*, 101.

(26) DMol^3; Molecular Simulations Inc: San Diego, CA, 1998.

(27) Perdew, J. P.; Wang, Y. *Phys. Rev.* **1992**, *B45*, 13244.

(28) Diagram produced with *Cerius^2 3.5*; Molecular Simulations Inc: San Diego, CA, 1997.

$-CH_2CH_2-$ grouping in the bedt-ttf layers on each side. Below the metal−insulator transition temperature the lattice conformation is resolved into two distinct sites. That is, all the bedt-ttf molecules have twisted−twisted conformations but one-quarter are staggered and the remainder are eclipsed. The C═C and C−S bond lengths within the ttf moieties are almost the same in both compounds at the temperatures investigated, so charge localization[13] can be ruled out as a reason for the different physical behavior. We believe this is the first example of a change in molecular conformation bringing about such large change in electrical properties in a molecular charge transfer salt. It also reveals the subtle influence of templating molecules on the structures and properties of this class of solid.

Acknowledgment. This work is supported by the UK Engineering and Physical Sciences Research Council (Research grant to P.D. and research studentship to L.M.) L.M. thanks Monbusho for financial assistance in visiting the Institute of Molecular Science in Okazaki. We thank Prof. Kyuya Yakushi of the Institute for Molecular Science for provision of the Raman facilities and helpful discussions.

Supporting Information Available: Crystallographic data is also available in CIF format. These materials are available free of charge via the Internet at http://pubs.acs.org.

IC990102U